Author's personal copy

Microelectronics Reliability 51 (2011) 1637–1639

Contents lists available at ScienceDirect

Microelectronics Reliability

journal homepage: www.elsevier.com/locate/microrel

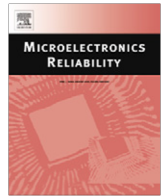

Chromatic and spherical aberration correction for silicon aplanatic solid immersion lens for fault isolation and photon emission microscopy of integrated circuits

B.B. Goldberg [a,e,*], A. Yurt [b], Y. Lu [c], E. Ramsay [a], F.H. Köklü [d], J. Mertz [e], T.G. Bifano [c,e], M.S. Ünlü [d,e]

[a] Department of Physics, Boston University, Boston, MA, USA
[b] Department of Materials Science and Engineering, Boston University, Boston, MA, USA
[c] Department of Mechanical Engineering, Boston University, Boston, MA, USA
[d] Department of Electrical and Computer Engineering, Boston University, Boston, MA, USA
[e] Centers for Nanoscience and Photonics, Boston University, Boston, MA, USA

A R T I C L E I N F O

Article history:
Received 1 June 2011
Received in revised form 11 July 2011
Accepted 13 July 2011
Available online 4 August 2011

A B S T R A C T

Current state-of-the-art in backside fault isolation and logic analysis utilizes solid immersion lens (SIL) imaging in the central configuration. An attractive advancement is the development and integration of an aplanatic SIL, which allows significant improvement in resolution, signal acquisition and isolation capabilities, especially for the 22 nm node and beyond. However, aplanatic SIL configurations introduce both chromatic and spherical aberrations. We have developed backing objective designs capable of correcting for chromatic aberrations allowing application in photon emission microscopy, as well as deformable mirror designs and experiments that eliminate spherical aberrations of aplanatic SILs to account for variations in substrate thickness and off-axis imaging.

© 2011 Elsevier Ltd. All rights reserved.

1. Introduction

Since their invention in 1990 [1] solid immersion lenses (SILs) have become widely used in the semiconductor failure analysis industry to improve resolution and signal collection for backside photon-based imaging techniques. SILs are generally of a plano-convex design, where the planar surface sits in optical contact with the substrate of the device under test (DUT) and the convex surface faces the backing objective in the imaging system. Two types of SIL geometries allow the possibility to perform aberration-free imaging. The first images light at the center of the radius of curvature of the immersion lens, and is known as a central SIL. The second images light at the aplanatic point of the immersion lens, a distance R/n below the center, and is known as an aplanatic SIL. In a perfect, on-axis, model system, both designs are aberration free. The aplanatic SIL also increases the numerical aperture of the imaging system, and is often referred to as a numerical aperture increasing lens, or NAIL [2].

When imaging areal device under test (DUT) with an immersion lens of either type, many factors lead to spherical aberrations: Off-axis imaging, errors in fabrication of the surfaces, and an unknown thickness of the substrate and distance from back surface to transistor level. Since spherical aberration free imaging is only possible if the region of interest sits at the center or aplanatic point of the SIL, any mismatch between the design thickness and the actual thickness of the substrate will rapidly cause an increase in the focus spot size. Several groups have studied spherical aberration correction in index mismatched materials using adaptive optics [3]. Here we report the use of adaptive optics for correction of aberrations due to a mismatch between the thickness of a central SIL and substrate.

Moving from a central to an aplanatic SIL also introduces chromatic aberrations, since the incoming rays are no longer perpendicular to the spherical lens surface. Photon emission microscopy (PEM) is a current state-of-the-art technique for the extraction of timing information from individual transistors on integrated circuits (ICs) that is critical in both device debug and failure analysis [4]. The reduction in feature size with the advent of advanced technology nodes will affect PEM imaging with respect to localization, photon flux and detection wavelength. Lower supply voltages to the IC will exponentially reduce the number of emitted photons per timing event, as well as shift the wavelength of emission further into the infrared, making detection more difficult [5].

An aplanatic solid immersion lens (ASIL) can maximize the collection efficiency of a PEM microscope with improvement in both lateral resolution as well as enhanced collection efficiency [2], at the expense of chromatic aberration due to dispersion of the ASIL [6]. The peak wavelength of photon emission varies according to

* Corresponding author at: Department of Physics, Boston University, Boston, MA, USA. Tel.: +1 617 353 5789; fax: +1 617 353 7271.
E-mail address: goldberg@bu.edu (B.B. Goldberg).

0026-2714/$ - see front matter © 2011 Elsevier Ltd. All rights reserved.
doi:10.1016/j.microrel.2011.07.047

Author's personal copy

the technology node as does the spectral bandwidth. To accommodate the range of wavelengths at maximum imaging power, we study the chromatic aberration behavior of a silicon ASIL in the spectral range 1.4–2.6 μm, particularly relevant to PEM [4]. We demonstrate that the inherent aberrations due to the silicon ASIL significantly degrade the imaging performance of a PEM microscope and these aberrations can be minimized by an accompanying corrective objective such that the imaging system benefits the full advantages of the ASIL for PEM techniques.

2. Experiment

2.1. Using deformable mirrors to correct spherical aberrations in a solid immersion lens

A continuous face-sheet MEMS-based deformable mirror (DM) with 140 electrostatic actuators (Boston Micromachines Corp.) was used to tailor the wavefront of the illumination light to compensate for spherical aberrations induced by an error in substrate thickness. The DM features 3.5 μm stroke and 400 μm pitch between actuators. In order to best control the phase profile of the illumination beam the DM was controlled in an open-loop fashion [7]. Measurements were made of the reflected spot size and reflected wavefront error, and these parameters were minimized using DM correction of the input beam. In these initial studies we used a central sapphire SIL to allow us to work in the visible. Future work will test with an aplanatic silicon SIL operating in the near-infrared.

The system was modeled in ZEMAX, with a perfect paraxial lens in lieu of an objective at the NA of the objective that we intended to use in our experiment: A Mitutoyo 20×, 0.4NA, infinity-corrected objective lens. Rays from this lens were focused through a sapphire SIL of radius of curvature of 2.38 mm and an index of refraction of 1.77. A 150 μm-thick slab of N-BK7 glass was placed between the SIL and the detector plane, and the system optimized to provide best focus. Fig. 1 shows the spot diagram obtained for this configuration; the black circle shows the Airy disk for this system. Clearly, the system is no longer diffraction limited. We then designed an experiment to attempt to correct for the induced aberration.

The optical setup schematic is shown in Fig. 2. Light from a helium–neon laser (HeNe) was directed from a DM (far right of figure) with an active aperture size of 3.6 mm to the pupil of the Mitutoyo infinity-corrected objective, shown on the left side of the figure. The DM surface was conjugated with the back pupil plane of the objective using a telescope with a magnification of 2. The objective focused the light at normal incidence onto a silvered mirror surface. The reflected light was then directed via a beamsplitter to two detectors; one a camera (CCD in figure) and the other a Shack-Hartmann wavefront sensor (WFS), positioned conjugate to the DM and the pupil plane. This configuration was used to make a baseline measurement of the aberration in the system. The sapphire SIL was then placed onto the surface of the mirror and fixed using a small bead of water, before light from the laser was focused to the center of the hemisphere. As expected, no increase in spherical aberration was seen in this configuration. Finally, we introduced a 150 μm thick glass cover slip between the SIL and mirror to create a non-optimal SIL/substrate combination. The system was then refocused onto the mirror surface and an analysis of the wavefront was made. This showed a dominant spherical aberration term in the wavefront. To correct for this, open-loop spherical aberration correction was applied using the DM. This increased the intensity by a factor of around 1.4, as can be seen in Fig. 3 and the rms wavefront error was also decreased by 30%. The wavefront error is the rms displacement of wavefront in the direction of beam propagation, as measured by the wave-

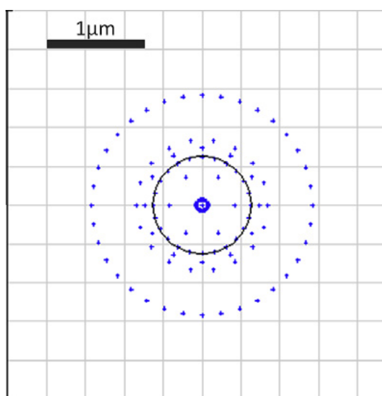

Fig. 1. Spot diagram when using a sapphire SIL and glass cover slip.

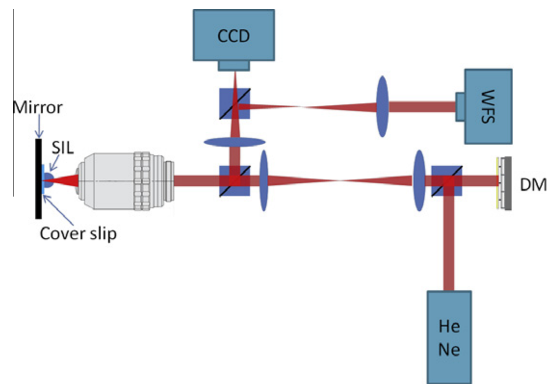

Fig. 2. Schematic of the optical setup for the sapphire SIL with cover slip.

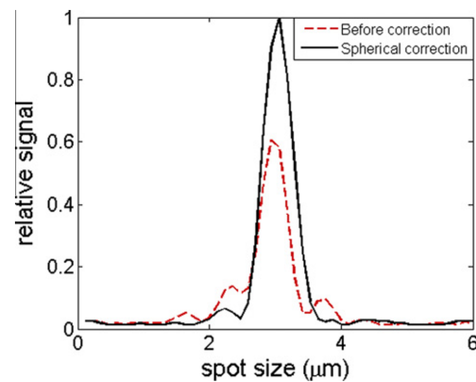

Fig. 3. Spherical aberration correction on the sapphire and cover slip.

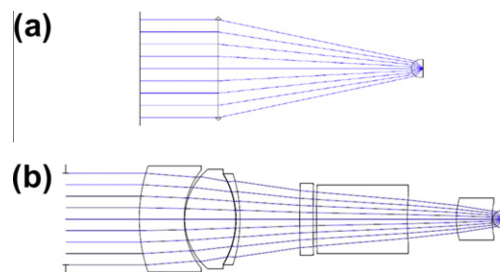

Fig. 4. Schematic of the designs (a) ASIL with perfect lens and (b) ASIL with corrective objective lens. The diameter of the SIL is 2.3 mm.

Author's personal copy

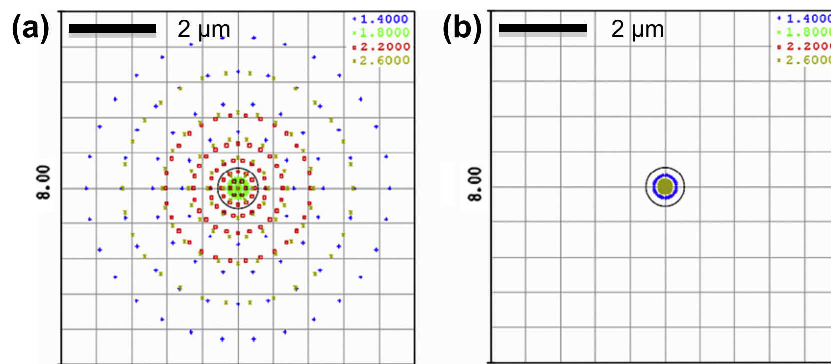

Fig. 5. Spot diagrams at focal plane for collimated beam of different wavelengths. (a) ASIL with perfect lens and (b) ASIL with corrective objective lens. The scale bar is 2 μm. The black circle denotes the Airy disk.

front sensor. This leads to a near-diffraction limited spot with low residual aberration. We have performed simulations in ZEMAX showing the effects of incorrect substrate thickness in the case of aplanatic silicon SILs. The spot diagrams for a 25 μm mismatch in substrate thickness show an increase in the lateral spot size by over an order of magnitude. We believe that using DMs it should be possible to correct for these aberrations.

2.2. Chromatic aberration correction design for aplanatic solid immersion lens

We created two designs for PEM imaging objective lenses in ZEMAX (see Fig. 4). The first design, shown in Fig. 4a, consisted of a perfect positive lens, free from aberration, focusing light through an ASIL to a point. This design allows us to understand the inherent chromatic aberration that exists due to the SIL dispersion. The second design is a corrected objective lens composed of six elements followed by the ASIL. This design minimizes both chromatic and monochromatic aberrations. To study the designs, a collimated polychromatic light beam that included an unweighted amplitude distribution of wavelengths between 1.4 μm and 2.6 μm was launched from the entrance pupil and the rays were traced through the optics to the image plane of the system. The image plane was assumed to be located on the planar surface of the ASIL and in homogenous silicon material. Both designs were constrained to have an effective numerical aperture (NA) of 2. This led to an average, diffraction limited resolution of about 350 nm in silicon across the entire spectrum of interest.

Without correction, the focal length of the imaging system varied by around 7 μm between wavelengths of 1.4 μm and 2.6 μm due to inherent chromatic aberration of the ASIL. For the corrected design, the chromatic focal shift was reduced to a maximum value of 330 nm over the entire spectrum, more than a factor of 20 improvement.

Fig. 5 shows the focal plane spot diagram for each lens design. Both Fig. 5a and b are to the same scale, with different colors corresponding to different wavelengths in the range considered. The black circle corresponds to the diffraction limited Airy disk. The uncorrected lens design (left) shows all rays (except the primary design wavelength of $\lambda = 1.8$ μm) were spread over the transverse focal plane over due to strong chromatic aberration. Conversely, all wavelength components were restricted to the Airy disk in the second design, thus providing for diffraction limited focusing across the full spectrum. For this study, both designs were constrained to a NA of 2 which was assumed sufficient for resolving the features of interest. A more stringent goal would be for higher NA which would include higher angle component of rays, which we are currently exploring.

3. Conclusions

We have performed open-loop correction using a deformable mirror to compensate for wavefront aberration in the central SIL configuration when the substrate thickness does not match that for which the SIL is designed. We have shown a reduction in rms wavefront error of 30% in sapphire. This work can be extended to use in silicon integrated circuits where silicon SILs may not be exactly matched to the substrate thickness in a device under test. In addition, we have demonstrated the effect of chromatic aberration of the ASIL on the imaging performance for PEM applications. Although ASIL provides significant improvement in terms of resolution and collection efficiency of photons, the aberrations must be corrected in order to take full advantage of ASIL in PEM microscopy in which the photon emission rate and device separation distance has been ever shrinking for state-of-the-art IC technology. We present a corrective objective design which eliminates the aberrations that exist in ASIL in order to achieve high-performance PEM imaging for fault detection and failure analysis of ICs has been proposed to fulfill the requirement of the-state-of-the-art IC technology.

Acknowledgment

The authors would like to acknowledge support from AFRL.

References

[1] Mansfield SM, Kino GS. Solid immersion microscope. Appl Phys Lett 1990;57(24):2615–6.
[2] Ippolito SB, Goldberg BB, Ünlü BB. High spatial resolution subsurface microscopy. Appl Phys Lett 2001;78(26):4071–3.
[3] Sherman L, Ye JY, Albert O, Norris TB. Adaptive correction of depth-induced aberrations in multiphoton scanning microscopy using a deformable mirror. J Microsc 2002;206:65–71;
Booth MJ, Neil MAA, Wilson T. Aberration correction for confocal imaging in refractive-index-mismatched media. J Microsc 1998;192:90–8;
Kner P, Sedat JW, Agard DA, Kam Z. High-resolution wide-field microscopy with adaptive optics for spherical aberration correction and motionless focusing. J Microsc 2009;237:136–47.
[4] Polonsky S, Bhushan M, Gattiker A, Weger A, Song P. Photon emission microscopy of inter/intra chip device performance variations. Microelectron Reliab 2005;45:1471Tosi A, Stellari F, Pigozzi A, Marchesi G, Zappa F. Hot-carrier photoemission in scaled CMOS technologies: a challenge for emission based testing and diagnostics. In: Reliability physics symposium proceedings, 2006. 44th annual, IEEE international; 2006. p. 595.
[5] Tam S, Chenming H. Hot-electron-induced photon and photocarrier generation in Silicon MOSFET's. IEEE Trans Electron Dev 1984;31:1264.
[6] Wang L, Pitter MC, Somekh MG. Wide-field high-resolution solid immersion fluorescence microscopy applying an aplanatic solid immersion lens. Appl Opt 2010;49:6160.
[7] Diouf A, LeGendre AP, Stewart JB, Bifano TG, Lu Y. Open-loop shape control for continuous microelectromechanical system deformable mirror. Appl Opt 2010;49(31):G148–54.